

## Role of 4*f* states in infinite-layer NdNiO<sub>2</sub>

Mi-Young Choi,<sup>1</sup> Kwan-Woo Lee <sup>1,2,\*</sup> and Warren E. Pickett <sup>3,†</sup>

<sup>1</sup>*Department of Applied Physics, Graduate School, Korea University, Sejong 30019, Korea*

<sup>2</sup>*Division of Display and Semiconductor Physics, Korea University, Sejong 30019, Korea*

<sup>3</sup>*Department of Physics, University of California, Davis, California 95616, USA*



(Received 7 November 2019; published 10 January 2020)

Atomic 4*f* states have been found to be essential players in the physical behavior of lanthanide compounds, at the Fermi level  $E_F$  as in the proposed topological Kondo insulator SmB<sub>6</sub>, or further away as in the magnetic superconductor system  $RNi_2B_2C$  ( $R$  = rare-earth ion) and in  $Y_{1-x}Pr_xBa_2Cu_3O_7$ , where the 4*f* shell of Pr has a devastating effect on superconductivity. In hole-doped  $RNiO_2$ , the  $R$  = Nd member is found to be superconducting while  $R$  = La is not, in spite of the calculated electronic structures being nearly identical. We report first-principles results that indicate that the Nd 4*f* moment affects states at  $E_F$  in infinite-layer NdNiO<sub>2</sub>, an effect that will not occur for LaNiO<sub>2</sub>. Treating 20% hole doping in the virtual crystal approach indicates that 0.15 holes empty the  $\Gamma$ -centered Nd-derived electron pocket while leaving the other electron pocket unchanged; hence Ni only absorbs 0.05 holes; the La counterpart would behave similarly. However, coupling of 4*f* states to the electron pockets at  $E_F$  arises through the Nd intra-atomic 4*f*-5*d* exchange coupling  $K \approx 0.5$ eV and is ferromagnetic (FM), i.e., anti-Kondo, in sign. This interaction causes spin-disorder broadening of the electron pockets and should be included in models of the normal and superconducting states of Nd<sub>0.8</sub>Sr<sub>0.2</sub>NiO<sub>2</sub>. The Ni moments differ by  $0.2\mu_B$  for FM and antiferromagnetic alignment (the latter are larger), reflecting some itineracy and indicating that Heisenberg coupling of the moments may not provide a quantitative modeling of Ni-Ni exchange coupling.

DOI: [10.1103/PhysRevB.101.020503](https://doi.org/10.1103/PhysRevB.101.020503)

### I. BACKGROUND AND MAJOR ISSUES

The discovery of superconductivity up to  $T_c = 15$  K in Sr-doped NdNiO<sub>2</sub> (Nd<sub>0.8</sub>Sr<sub>0.2</sub>NiO<sub>2</sub>) [1] has reinvigorated the three-decade-long issue of whether there may be nickelates that can host cuprate-type superconductivity. LaNiO<sub>2</sub>, which is isostructural with “infinite layer” CaCuO<sub>2</sub> [2] that superconducts up to 110 K when doped [3], has been one of the prime candidates, but what doping is possible has never resulted in superconductivity. NdNiO<sub>2</sub> is also isovalent with CaCuO<sub>2</sub>, providing a nominal  $d^9$  configuration on the open shell transition metal ion.

Early comparison of the electronic structures of CaCuO<sub>2</sub> and NdNiO<sub>2</sub> identified similarities but substantial differences [4,5], with questions about whether concepts such as strong superexchange coupling of the transition metal moments, or of Zhang-Rice singlets upon doping [1], are relevant to this nickelate. A number of groups recently have revisited this question, with the objective of few-band model building to quantify differences related to superconductivity [6–19]. The popular approach has been to obtain the nonmagnetic local density approximation (LDA) band structure of NdNiO<sub>2</sub> with the 4*f*<sup>3</sup> electrons assigned to a nonmagnetic core, then approximate the low-energy bands with a minimal local orbital model, add a repulsive local interaction, and evaluate the consequences, viz., the pairing susceptibility. Close attention is given to the geometry of the Fermi surface (FS), which strongly impacts the pairing susceptibility.

Detailed analyses of the LDA electronic structure have been provided by Botana and Norman [6] for LaNiO<sub>2</sub> and by Nomura *et al.* [9] for NdNiO<sub>2</sub>, in which three nonmagnetic 4*f* electrons are included in the Nd core. In addition to the roughly half-filled Ni 3*d*<sub>*x*<sup>2</sup>-*y*<sup>2</sup></sub> band, several groups find and quantify Nd 5*d*-derived bands obtained earlier [4,5]. A Nd 5*d*<sub>*z*<sup>2</sup></sub> band drops below the Fermi level  $E_F$  at  $\Gamma$ , and in addition a band usually identified as Nd 5*d*<sub>*xy*</sub>-derived drops below  $E_F$  at the zone corner  $A = (\pi, \pi, \pi)$  point [in units of  $(\frac{1}{a}, \frac{1}{a}, \frac{1}{c})$ ]. This undoped NdNiO<sub>2</sub> FS differs in significant ways from that of nonmagnetic CaCuO<sub>2</sub> but is similar to LaNiO<sub>2</sub>. X-ray absorption spectra of the O  $K$  and Ni  $L_3$  edges [20] do not reveal significant differences between LaNiO<sub>2</sub> and NdNiO<sub>2</sub>.

There are other fundamental questions to be considered. Experimentally, undoped CaCuO<sub>2</sub> orders antiferromagnetically with a high Néel temperature of 442 K [21], while undoped NdNiO<sub>2</sub> and LaNiO<sub>2</sub> do not order [1]. The underlying differences with cuprates are several. The mean Ni 3*d* level  $\epsilon_d$  is separated from the O 2*p* level  $\epsilon_p$  by 4 eV in the nickelates versus only 2 eV in the cuprate [6]. Ni therefore has less hybridization with oxygen 2*p* orbitals than does Cu, thus should have a stronger tendency toward local moment magnetism than does Cu, and indeed it does so in LDA calculations. The superexchange coupling  $J$  is much smaller for the nickelate [6], thus one expects a lower but nonzero Néel temperature. Finally, LaNiO<sub>2</sub> and NdNiO<sub>2</sub> are reported as conducting (albeit poorly), whereas CaCuO<sub>2</sub> is insulating. Lack of Ni ordering is a central question to address; however, both in calculations and experimentally the nickelates are conducting. We note that magnetic order disappears in cuprates when they are doped to become conducting.

\*mckwan@korea.ac.kr

†wepickett@ucdavis.edu

The model treatments mentioned above would suggest that doped  $\text{LaNiO}_2$  should be superconducting as is doped  $\text{NdNiO}_2$ . Since this is not the case, we pursue the viewpoint that a more fundamental question is what features may account for this difference between two highly similar nickelates. La and Nd are very similar chemically, with tripositive ionic radii only slightly larger for La than for Nd. Although small size differences in lattice constants or strains can influence states in correlated insulators, itinerancy and screening by carriers strongly reduce such effects.

An obvious difference between these nickelates is that  $\text{La}^{3+}$  is closed shell and nonmagnetic, whereas  $\text{Nd}^{3+}$ , with Hund's rule ground state  $S = \frac{3}{2}$ ,  $L = 6$ ,  $J = \frac{9}{2}$ , has a (free ion) Curie-Weiss moment of nearly  $4\mu_B$ . Superconductivity appears in  $\text{Nd}_{0.8}\text{Sr}_{0.2}\text{NiO}_2$  in the midst of these large disordered local moments, which should compete with superconducting phases, directly or by introducing disorder into the electronic structure. In several YBCO-type cuprates, however, replacing a nonmagnetic rare-earth ion (La or Y) by a magnetic lanthanide from Dy to Tb does not affect the superconductivity, because the small  $4f$  orbital is not involved in the electronic structure. Surprisingly,  $\text{PrBa}_2\text{Cu}_3\text{O}_7$  was found to be non-superconducting [22], due to antibonding coupling of the Pr  $4f_{z(x^2-y^2)}$  orbital to the O  $2p$  orbitals [23,24]. Notably, the local environment of the  $4f$  ion is the same as in  $\text{NdNiO}_2$ .

Another related system is the rare-earth nickel borocarbides  $R\text{Ni}_2\text{B}_2\text{C}$  where  $R$  can be one of many of the rare-earth atoms. This system displays strong interplay and competition between the  $R$   $4f$  magnetic moment and the conduction states with heavy Ni character, with the  $R$   $5d$  playing an important role in coupling the local moments to the itinerant states [25,26]. Elemental europium at high pressure but retaining a  $f^7$  local moment, switches from metallic and magnetically ordered to superconducting and magnetically disordered around 80 GPa [27,28], providing its own questions about the effect of  $4f$  moments on pairing, a coupling that must proceed through the Eu  $5d$  states.

The question of possible impact of the  $4f$  shell has not been addressed in  $\text{NdNiO}_2$ . While direct  $4f$ -nickelate hybridization may be small, there is an intra-atomic exchange coupling between the  $4f$  spin and the  $5d$  states around  $E_F$  that, as mentioned, does not occur in  $\text{LaNiO}_2$ . Since the  $5d$  bands cross  $E_F$ , carriers will be affected. Specifically, with disordered Nd moments, the  $5d$  on-site energies will be spin split, with a projection along any given direction that is distributed randomly. A carrier in a  $5d$  band will be subjected to a random potential, resulting in band broadening and magnetic scattering that is absent in  $\text{LaNiO}_2$ .

The presentation is organized as follows. The computational methods and material configurations are described in Sec. II. In Sec. III results are presented for four assumed types of magnetic order in  $\text{NdNiO}_2$ . The electronic bands and Fermi surfaces for nonmagnetic Ni are discussed in Sec. IV. A few results relating to the occupied Nd  $4f$  orbitals are presented in Sec. V, followed by a discussion of hole doping in Sec. VI. Some observations about the effects of magnetic order and relation to other  $4f$ -containing superconductors are made in Sec. VII, which is followed by a brief summary in Sec. VIII.

## II. COMPUTATIONAL METHODS

We have studied the electronic and magnetic properties of  $\text{NdNiO}_2$  using the precise, all-electron, full potential linearized augmented plane-wave method as implemented in WIEN2K [29]. The lattice constants  $a = 3.92 \text{ \AA}$ ,  $c = 3.37 \text{ \AA}$  observed for superconducting  $\text{Nd}_{0.8}\text{Sr}_{0.2}\text{NiO}_2$  [1] have been used; all atoms lie at  $P4/mmm$  symmetry determined positions. Strong intra-atomic interactions on Nd, and usually on Ni in nickelates, are modeled with the DFT +  $U$  method [30] (density functional theory plus Hubbard  $U$ ), which is essential to preserve the  $4f$  local moment and place the corresponding bands away from  $E_F$ . The fully anisotropic, rotationally invariant DFT +  $U$  correlation correction functional in the fully localized limit form [31] implemented in WIEN2K, was used. Results are presented for  $U_f^{\text{Nd}} = 8.0 \text{ eV}$ ,  $J_f^{\text{Nd}} = 1.0 \text{ eV}$ ,  $U_d^{\text{Ni}} = 5.0 \text{ eV}$ , and  $J_d^{\text{Ni}} = 0.7 \text{ eV}$  (and occasionally for  $U_d^{\text{Ni}} = 0$ ). Other input parameters and a survey of results beyond those presented here are provided in the Supplemental Material (SM) [32]. Section VI was carried out by reducing the nuclear charge on Nd by 0.20, and removing the same amount of electrons.

The strong local  $4f$  moment requires magnetically ordered calculations. We find that Ni prefers a moment of the order of  $0.5\mu_B$  without any  $U^{\text{Ni}}$ , which increases to  $\sim 1\mu_B$  for the values we have used. The Nd moment always assumes the spin value of  $3\mu_B$  characteristic of an  $f^3$  Hund's rule ion, plus minor exchange polarization of the  $5d$  orbitals. We have studied four magnetic configurations:

AFM0: antiferromagnetic (AFM) Nd layers with nonmagnetic Ni layers;

AFM1: both Ni and Nd layers have antialigned moments;

AFM2: ferromagnetic (FM) Nd layers and AFM Ni layers; and

FM: all Nd and Ni moments aligned.

Note that it is the AFM1 and AFM2 cases in which Ni is antiferromagnetically ordered. Note also that AFM0 is done with  $U_d^{\text{Ni}} = 0$ , so its energy cannot be compared with the other cases.

The SM provides additional information about the electronic structures. An insulating band structure is never obtained, which is a great difference compared with cuprates. It was shown earlier that increasing  $U$  on Ni in  $\text{NdNiO}_2$  never leads to a Mott insulator; instead a  $3d_{z^2}$  orbital becomes unoccupied and forms a peculiar intra-atomic singlet with the  $d_{x^2-y^2}$  orbital [5].

## III. MAGNETIC ORDER

Although it is expected that  $\text{Ni}^{1+} d^9$  ions will tend to order in antiferromagnetic (AFM1 or AFM2) fashion through superexchange as does  $\text{CaCuO}_2$  and several other  $d^9$  cuprates, we begin with FM alignment within both Ni and Nd layers, as it enables identification of the intra-atomic exchange splitting between the occupied Nd  $4f$  and conduction  $5d_{z^2}$  orbitals.

A magnetic Ni ion leads to a 120 meV energy gain compared to nonmagnetic. This exaggerated tendency toward magnetic ordering and the magnitude of the magnetic moment are a known deficiency of (semi) local density functional

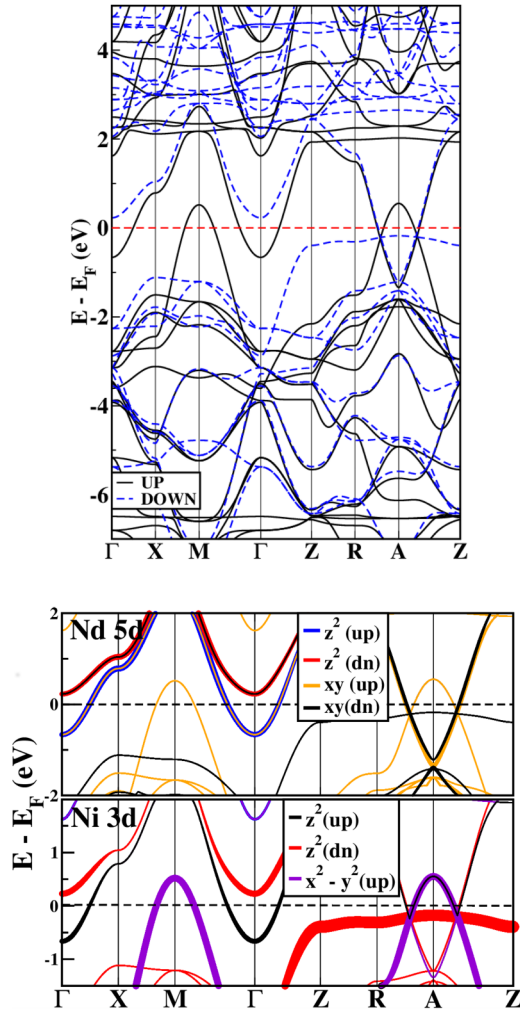


FIG. 1. Top: GGA +  $U$  FM bands of NdNiO<sub>2</sub>: solid lines denote majority, dashed lines indicate minority, and  $E_F$  is the zero of energy. Bottom: Color fatband plot of FM NdNiO<sub>2</sub> near  $E_F$ , with the legend describing the color choice. Note the Nd-derived electron pockets at  $\Gamma$  and  $A$ , and the Ni majority  $d_{x^2-y^2}$  hole pockets at  $M$  and  $A$ .

methods, with much of the problem attributed to the lack of effects of spin fluctuations in the functional.

The energies can be compared for those cases with magnetic Ni (AFM1, AFM2, FM) for which the same functional is used. The energy of AFM2 (FM Nd) is slightly lower than that of AFM1 (AFM Nd), by 7 meV for  $U^{\text{Ni}} = 0$  and by only 1 meV (at the edge of computational precision) with  $U^{\text{Ni}} = 5$  eV, reflecting a slight tendency toward FM ordering of the 4f moments. The energy difference between FM and AFM2 provides the difference between AFM and FM Ni moment alignment; AFM is favored by 116 (25) meV/Ni in GGA(+ $U$ ). This energy difference contains information about Ni-Ni in-plane exchange coupling, and would give a value of the nearest-neighbor coupling if more distant exchange couplings were negligible. Liu *et al.* have derived values of coupling for a few neighbors, concluding that the values depend strongly on the value of  $U^{\text{Ni}}$  that is assumed [18].

For the FM bands shown in Fig. 1 the Ni and Nd moments are aligned into an overall FM structure. The Ni  $d_{x^2-y^2}$  bands that give rise to the large FS are spin split by 2 eV, reflecting

the Ni spin moment of order  $1\mu_B$ . As noted earlier [4,5] and recently by several others, Nd 5d-derived bands dip below  $E_F$  at the zone center  $\Gamma$  and at the zone corner  $A$ , with bonding  $5d_{z^2}$  and antibonding  $5d_{xy}$  character, respectively [9]. There is mixing with Ni  $d_{z^2}$  in both of these electron pockets, especially the latter. This mixing is due to the surprise that the minority (but occupied) Ni  $d_{z^2}$  antibonding band at  $k_z = \pi$  (see the Z-R-A-Z lines) lies within 0.2–0.4 eV of  $E_F$ .

As shown in Fig. 1, the  $5d_{z^2}$  band energies relative to  $E_F$  of up (down) bands are  $-0.7(+0.3)$  eV at  $\Gamma$ , giving an intra-atomic coupling  $H^{\text{Nd}} = K\hat{e}_{4f} \cdot \hat{e}_{5d}$  with  $K = 0.5$  eV, in terms of the orientations of the 4f and 5d spins. For the antibonding  $5d_{xy}$  orbital the eigenvalues at  $A$  lie at  $-1.2$  eV with a splitting of less than 0.1 eV, reflecting the participation of Ni 3d orbitals and the out-of-phase character of states at the  $A$  point. Note that this coupling is Hund’s rule alignment of 4f and 5d states and therefore anti-Kondo coupling of the local moment to the conduction band, as opposed to some suggested Kondo modeling of Nd<sub>0.8</sub>Sr<sub>0.2</sub>NiO<sub>2</sub> [4,20]. Such anti-Kondo coupling has been studied in other lanthanide compounds [33]. We return below to the  $K \approx 0.5$  eV intra-atomic exchange coupling of Nd 5d states.

#### IV. NONMAGNETIC Ni AND FERMI SURFACES

Low-energy models of oxides including superconducting possibilities are based on nonmagnetic Ni, with an on-site repulsion added to provide correlated electron behavior and a potential pairing mechanism. We have obtained a DFT +  $U$  solution with nonmagnetic Ni ( $U_d^{\text{Ni}} = 0$ ,  $U_f^{\text{Nd}} = 8$  eV), our case AFM0. The Nd 4f moment that must remain fully spin polarized has AFM alignment, so the Brillouin zone is correspondingly folded back. The Ni moment for AFM alignment is  $1.2\mu_B$ , compared to  $1.0\mu_B$  for FM alignment. For  $U = 0$  (just GGA) the calculated moments are  $0.52\mu_B$  (AFM) and  $0.35\mu_B$  (FM); i.e., there is about  $0.2\mu_B$  difference in the moments, and the associated Hund’s energy would be an important contribution to the lower energies for AFM alignment.

The bands, density of states, and fatbands near  $E_F$  for AFM0 alignment are shown in Fig. 2, with symmetry points in that folded tetragonal zone now designated with primes. Gaps at the zone boundaries indicate effects of the Nd AFM order, e.g., a gap of 0.3 eV can be seen in the Nd 5d band around 0.8 eV at  $X'$ . As for the FM order above, this splitting vanishes for the corresponding antibonding band at  $R'$ . The nearby folded Ni 3d band displays no gap, reflecting canceling mixing with the eight neighboring Nd sites.

The bands crossing  $E_F$  giving the FSs are those that are fit to few band models. The corresponding FSs are shown in Fig. 3. The Nd  $5d_{z^2}$  related electron pocket Pk1 at  $\Gamma$  has attracted attention, with the electron pocket Pk2 at  $A = (\pi, \pi, \pi)$  ( $Z'$  in Fig. 2) also receiving notice. Pk2 has strong Ni  $3d_{z^2}$  character as well as some  $3d_{xz,yz}$  influence, considerably stronger than the Nd  $5d_{xy}$  component that has been discussed by several groups [5–10]. Due to  $k_z$  dispersion, the large Ni  $d_{x^2-y^2}$  FS appears in this folded zone as a large banana centered at  $M'$ , and strongly fluted cylinders also centered at  $M'$  and connected by tiny necks at the corner  $R'$  points. These two surfaces are degenerate along the zone faces reflecting simple folding back into the AFM zone, and

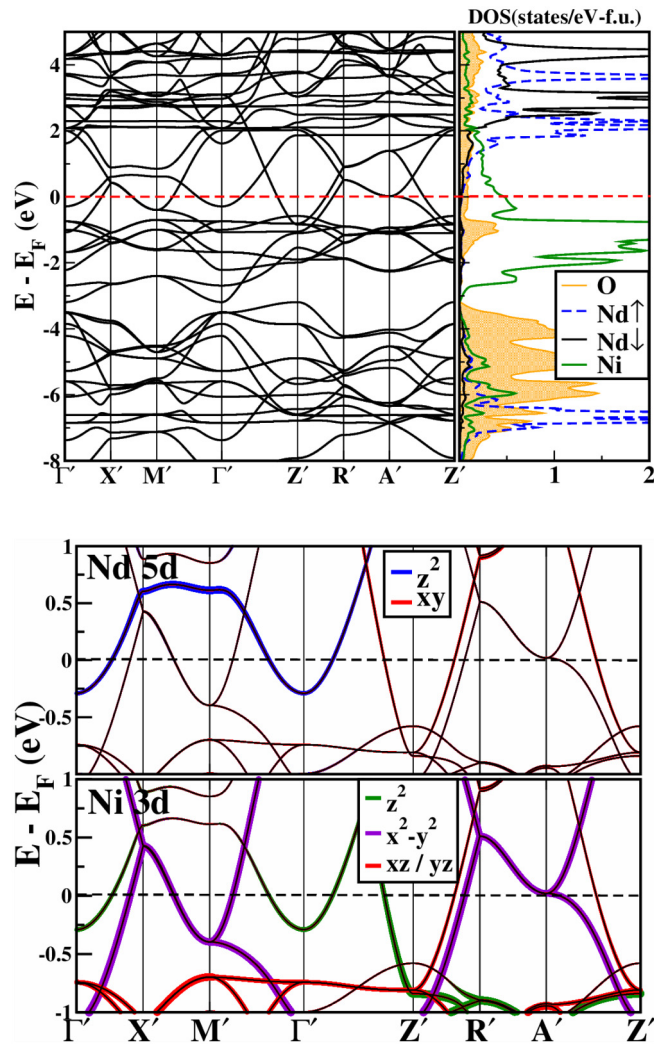


FIG. 2. Top: Bands of  $\text{NdNiO}_2$ , with AFM Nd moments and nonmagnetic Ni layer, plotted along lines in the AFM zone. Bottom: Fatbands indicating Nd  $5d$  character (above) and Ni  $3d$  weight (below), with orbital character as noted. In terms of the usual  $\text{NiO}_2$  sublattice, the  $M$  ( $A$ ) point is folded back to  $\Gamma'$  ( $Z'$ ). The other symmetry points are  $X' = (\pi/2, \pi/2, 0)$  and  $M' = (\pi, 0, 0)$ , while  $R'$  and  $A'$  lie above these points by  $(0, 0, \pi)$ , respectively.

correspond to  $M$ -centered hole barrels in the primitive zone that are familiar from cuprate physics. These barrels have surprisingly large  $k_z$  dispersion, lessening the relevance of two-dimensional physics.

### V. OCCUPIED $4f$ ORBITALS

We now consider briefly the Nd  $4f$  contributions to the electronic and magnetic structure. The  $S = \frac{3}{2}$  spin configuration is strongly enforced by Hund's first rule, and the energy difference between FM and AFM order of the Nd moments is very small;  $\sim 7$  meV/Nd ion for Ni treated in GGA, and only 1 meV/Nd ion for Ni treated in GGA +  $U$ . The three occupied bands lie at  $-7$  eV with some small dispersion due to the direct overlap of  $4f$  and O  $2p$  orbitals, which is small but provides crystal field splitting of the  $4f$  orbitals. The occupied states that we obtained are combinations of  $m_\ell = -3, -2, +1$ , each

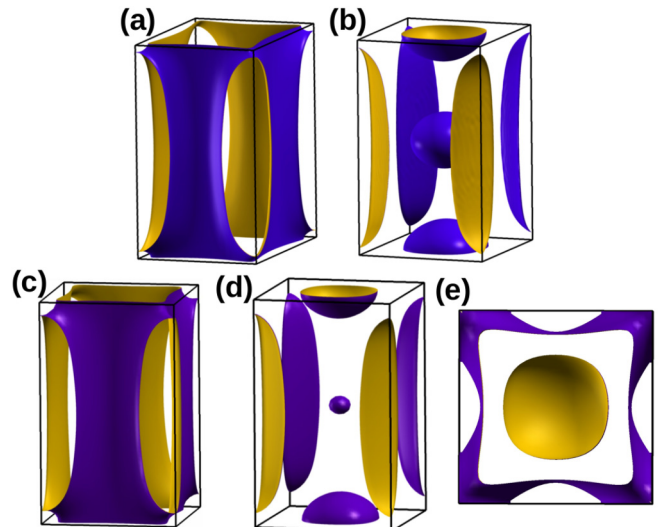


FIG. 3. Fermi surfaces for case AFM0 (nonmagnetic Ni), in the full zone corresponding to AFM  $4f$  alignment. Surfaces have been separated into left and right subpanels for clarity. (a),(b) Undoped  $\text{NdNiO}_2$ . The spheres are (i) the Nd  $5d$  electron pocket at  $\Gamma' = \Gamma$ , at the center of the figure, and (ii) the other electron pocket at  $A$  folded back to  $Z'$  (see text). (c),(d) Surfaces for VCA  $\text{Nd}_{0.8}\text{Sr}_{0.2}\text{NiO}_2$ ,  $x = 0.20$  hole doping. The  $\Gamma$ -centered electron pocket is essentially emptied, while the  $Z'$ -centered pocket is almost unchanged. (e) Top view of the  $\text{Nd}_{0.8}\text{Sr}_{0.2}\text{NiO}_2$  surfaces, showing the amount of  $k_z$  dispersion.

with lesser admixtures of  $+1, +2, -3$  states, respectively, with total orbital moment  $m_{orb} = 4.47\mu_B$ . When spin-orbit coupling is included, the occupied orbitals are those with  $j = \frac{5}{2}$ ,  $m_j = -\frac{5}{2}, -\frac{3}{2}, +\frac{1}{2}$ . (See SM for further information on these occupations.) The four unoccupied  $4f$  bands are centered 3.5 eV above  $E_F$  but are spread by the anisotropy of the orbitals and mixing with Nd  $5d$  states over a range of 3 eV.

### VI. HOLE DOPING

$\text{NdNiO}_2$  becomes superconducting upon hole doping by 0.2 hole/f.u. [1]. With the Fermi level density of states  $N(0) = 0.70/(\text{eV cell})$ , the drop in  $E_F$  (in rigid band) is 0.29 eV, which is enough to empty the Pk1 pocket at  $\Gamma$  to 0.4 eV, and to reduce the carrier density of Pk2 but leaving substantial Ni carriers. Rigid band treatment may be deceptive, however, due to Fermi level charge on both Ni and Nd atoms. We applied the virtual crystal approximation [34] (VCA) to obtain a more realistic effect of doping.

Fermi surfaces Pk1 and Pk2 of undoped [Figs. 3(a) and 3(b)] and  $x = 0.20$  doped  $\text{NdNiO}_2$  [Figs. 3(c)–3(e)] reveal important nonrigid band behavior, and the corresponding bands provided in Fig. 4 indicate the reason. The Ni  $d$  bands are shifted only slightly ( $\sim 0.1$  eV) with respect to  $E_F$  by doping, as is the band giving the  $A$ -centered pocket (at  $Z'$  in this figure). The Nd  $5d$  band at  $\Gamma$  is, however, shifted by 0.3 eV and effectively emptied of its (undoped) 0.15 electrons. These VCA bands are similar to the VCA bands of Sakakibara *et al.* [7] for  $\text{La}_{0.8}\text{Ba}_{0.2}\text{NiO}_2$ , a difference being that their La  $5d$  band is 0.2 eV higher than our Nd  $5d$  band.

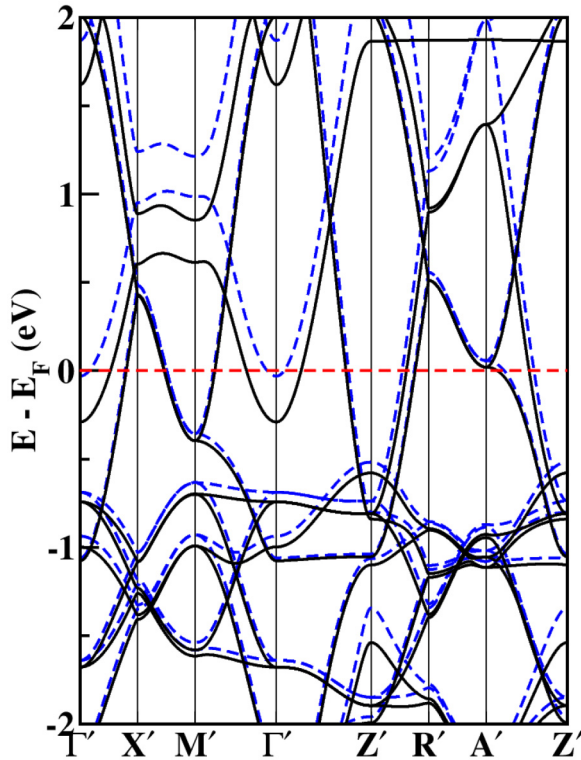


FIG. 4. Band structures of  $\text{Nd}_{0.8}\text{Sr}_{0.2}\text{NiO}_2$  (dashed lines) compared to those of  $\text{NdNiO}_2$  (solid lines), near  $E_F$ . Here  $U_d^{\text{Ni}} = 0$ ; Ni is nonmagnetic. The bands are plotted in the Nd AFM zone. Note that hole doping removes electrons primarily from the  $\Gamma$ -centered Nd  $5f$  electron pocket; the  $Z'$  ( $A$  in primitive zone) pocket is nearly unchanged.

The band giving rise to Pk2, often referred to as Nd  $5d_{xy}$ , is also heavily Ni in character (shown above, and in the SM), hence little affected as are the other Ni  $3d$  bands. The result is that  $x = 0.20$  doping changes the Ni  $3d$  charge by only 0.05 holes. The disappearance of pocket Pk1 and its associated disorder scattering may contribute to the drop in resistivity by a factor of 2–3 upon doping [1].

### VII. IMPLICATION OF SPIN DISORDER

The exchange splitting of the Nd  $5d$  band at  $\Gamma$  (near  $E_F$ ) reflects the intra-atomic  $4f$ - $5d$  exchange on Nd of  $K \approx 0.5$  eV. The  $S = \frac{3}{2}$  spin moment on Nd drives this exchange splitting, which will follow the orientation of the  $4f$  moment, which is disordered. With the very weak  $4f$ - $4f$  exchange coupling noted in Sec. III, the Nd moments will be randomly oriented and quasistatic on an electronic timescale.

In spite of the disorder broadening on the electron Fermi pockets and resulting strong spin scattering driven by stable, essentially classical but disordered  $4f$  moments, superconductivity survives in  $\text{Nd}_{0.8}\text{Sr}_{0.2}\text{NiO}_2$ . This situation bears some similarity to that of elemental Eu with its  $4f^7$  moment: pressure kills magnetic order around 82 GPa but not the local moment, and there is a first-order electronic but isostructural transformation to a superconducting phase at 1.7 K [27]. The exchange coupling from the classical local moment that

should be disruptive to Cooper pairing in a specific spin configuration (singlet or triplet) may actually be contributing to the pairing in Eu [28]. The exchange coupling in  $\text{NdNiO}_2$  is not as pervasive—every site in Eu has a  $4f$  moment and the partially occupied conduction band is entirely  $5d$ —but some of the physics may be related.

A related, and commonly modeled, spin-scattering process will occur on the (locally) magnetic Ni ion (as treated for the Cu ion in cuprates), an effect that can be modeled by any of a variety of spin fluctuation formalisms applicable to transition metal oxides. The resulting strong scattering in the electron pockets is a potential contributor to the resistivity of “conducting”  $\text{NdNiO}_2$ , where the resistivity  $\rho \sim 1$  m $\Omega$  cm varies little between 300 K and the lowest temperature measured. The inferred mean free path in a Fermi liquid inspired Bloch-Boltzmann treatment would be atomic size, meaning incoherent transport and a washed out FS. A dynamical mean-field approximation treatment of Ni  $3d$  fluctuations [11] in  $\text{LaNiO}_2$  found little shifting and broadening of bands around  $E_F$ , and no mechanism for the high resistivity. The large residual resistivity may be the result of the topotactic synthesis technique, with indications to be learned between the similarities and the distinctions between the doped thin films and doped bulk materials [35], which also have similarly high residual resistivity.

### VIII. SUMMARY

In this work we have focused on a primary distinction between  $\text{NdNiO}_2$  and  $\text{LaNiO}_2$ . When the  $4f$  moment on Nd is relegated to the core in nonmagnetic fashion, the electronic structures are nearly identical. Yet the Nd compound becomes superconducting while the sister La compound remains nonsuperconducting, when 20% hole doped. We find that the strong Nd  $4f$  moment is intra-atomic exchange coupled to the Nd  $5d$  orbitals by a coupling of roughly  $K = 0.5$  eV, giving anti-Kondo coupling between the Nd local moments and the lower conduction band. The disordered  $4f$  moments will give rise to a broadening of  $5d$  bands of the order of  $K$ , affecting transport and perhaps becoming implicated in pairing, either as a participant or a disruptive agent.

The calculated Ni moments are larger by  $0.2\mu_B$  for antiferromagnetic alignment than for ferromagnetic alignment. The associated Hund’s rule energy provides a tendency toward AFM alignment that lies beyond the usual Heisenberg exchange coupling picture. An important feature of this system is that the  $\Gamma$ -centered Nd  $5d$  Fermi surface pocket accepts most of the doped holes, leaving Ni  $3d$  charge changed only by 0.05 holes for 20% doping. The Pk2 spherical Fermi surface pocket that remains intact after doping, and rather strong  $k_z$  fluting of the Ni Fermi surfaces, suggests the importance of  $k_z$  dispersion (three-dimensionality). Our results indicate that several aspects of the Nd ion arising from the open  $4f$  shell require attention for understanding both normal and superconducting state properties.

*Note added.* Recently, a useful discussion related to this work appeared in Ref. [36].

## ACKNOWLEDGMENTS

We acknowledge informative discussions with A. S. Botana, J. Sun, M. J. Han, E.-G. Moon, D. Lee, and J.

Son, and communication with S. Raghu. M.Y.C. and K.W.L. were supported by National Research Foundation of Korea Grant No. NRF-2019R1A2C1009588. W.E.P. was supported by NSF Grant No. DMR 1607139.

- [1] D. Li, K. Lee, B. Y. Wang, M. Osada, S. Crossley, H. R. Lee, Y. Cui, Y. Hikita, and H. Y. Hwang, Superconductivity in an infinite-layer nickelate, *Nature (London)* **572**, 624 (2019).
- [2] T. Siegrist, S. M. Zahurak, D. W. Murphy, and R. S. Roth, The parent structure of the layered high-temperature superconductors, *Nature (London)* **334**, 231 (1988).
- [3] M. Azuma, Z. Hiroi, M. Takano, Y. Bando, and Y. Tekeda, Superconductivity at 110 K in the infinite-layer compound  $(\text{Sr}_{1-x}\text{Ca}_x)_{1-y}\text{CuO}_2$ , *Nature (London)* **356**, 775 (1992).
- [4] V. I. Anisimov, D. Bukhvalov, and T. M. Rice, Electronic structure of possible nickelate analogs to the cuprates, *Phys. Rev. B* **59**, 7901 (1999).
- [5] K.-W. Lee and W. E. Pickett, Infinite-layer  $\text{LaNiO}_2$ :  $\text{Ni}^{1+}$  is not  $\text{Cu}^{2+}$ , *Phys. Rev. B* **70**, 165109 (2004).
- [6] A. S. Botana and M. R. Norman, Similarities and differences between infinite-layer nickelates and cuprates and implications for superconductivity, [arXiv:1908.10946](https://arxiv.org/abs/1908.10946) [*Phys. Rev. X* (to be published)].
- [7] H. Sakakibara, H. Usui, K. Suzuki, T. Kotani, H. Aoki, and K. Kuroki, Model construction and a possibility of cuprate-like pairing in a new  $d^9$  nickelate superconductor  $(\text{Nd}, \text{Sr})\text{NiO}_2$ , [arXiv:1909.00060](https://arxiv.org/abs/1909.00060).
- [8] X. Wu, D. D. Sante, T. Schwemmer, W. Hanke, H. Y. Hwang, S. Raghu, and R. Thomale, Robust  $d_{x^2-y^2}$ -wave superconductivity of infinite-layer nickelates, [arXiv:1909.03015](https://arxiv.org/abs/1909.03015).
- [9] Y. Nomura, M. Hirayama, T. Tadano, Y. Yoshimoto, K. Nakamura, and R. Arita, Formation of 2D single-component correlated electron system and band engineering in the nickelate superconductor  $\text{NdNiO}_2$ , *Phys. Rev. B* **100**, 205138 (2019).
- [10] J. Gao, Z. Wang, C. Fang, and H. Weng, Electronic structures and topological properties in nickelates  $\text{Ln}_{n+1}\text{Ni}_n\text{O}_{2n+2}$ , [arXiv:1909.04657](https://arxiv.org/abs/1909.04657).
- [11] S. Ryee, H. Yoon, T. J. Kim, M. Y. Jeong, and M. J. Han, Induced magnetic two-dimensionality by hole doping in superconducting  $\text{Nd}_{1-x}\text{Sr}_x\text{NiO}_2$ , [arXiv:1909.05824](https://arxiv.org/abs/1909.05824).
- [12] G.-M. Zhang, Y.-F. Yang, and F.-C. Zhang, Self-doped Mott insulator for parent compounds of nickelate superconductors, [arXiv:1909.11845](https://arxiv.org/abs/1909.11845).
- [13] H. Zhang, L. Jin, S. Wang, B. Xi, X. Shi, F. Ye, and J.-W. Mei, Effective Hamiltonian for superconducting Ni oxides  $\text{Nd}_{1-x}\text{Sr}_x\text{NiO}_2$ , [arXiv:1909.07427](https://arxiv.org/abs/1909.07427).
- [14] Y.-H. Zhang and A. Vishwanath, Kondo resonance and  $d$ -wave superconductivity in the  $t$ - $J$  model with spin one holes: Possible applications to the nickelate superconductor  $\text{Nd}_{1-x}\text{Sr}_x\text{NiO}_2$ , [arXiv:1909.12865](https://arxiv.org/abs/1909.12865).
- [15] P. Jiang, L. Si, Z. Liao, and Z. Zhong, Electronic structure of rare-earth infinite-layer  $\text{RNiO}_2$  ( $R = \text{La}, \text{Nd}$ ), *Phys. Rev. B* **100**, 201106(R) (2019).
- [16] L.-H. Hu and C. Wu, Two-band model for magnetism and superconductivity in nickelates, *Phys. Rev. Res.* **1**, 032046(R) (2019).
- [17] P. Werner and S. Hoshino, Nickelate superconductors: Multi-orbital nature and spin freezing, *Phys. Rev. B* **101**, 041104(R) (2020).
- [18] Z. Liu, Z. Ren, W. Zhu, Z. F. Wang, and J. Yang, Electronic and magnetic structure of infinite-layer  $\text{NdNiO}_2$ : Trace of antiferromagnetic metal, [arXiv:1912.01332](https://arxiv.org/abs/1912.01332).
- [19] M. Jiang, M. Berciu, and G. A. Sawatzky, Doped holes in  $\text{NdNiO}_2$  and high- $T_c$  cuprates show little similarity, [arXiv:1909.02557](https://arxiv.org/abs/1909.02557).
- [20] M. Hepting, D. Li, C. J. Jia, H. Lu, E. Paris, Y. Tseng, X. Feng, M. Osada, E. Been, Y. Hikita, Y.-D. Chuang, Z. Hussain, K. J. Zhou, A. Nag, M. Garcia-Fernandez, M. Rossi, H. Y. Huang, D. J. Huang, Z. X. Shen, T. Schmitt, H. Y. Hwang, B. Moritz, J. Zaanen, T. P. Devereaux, and W. S. Lee, Electronic structure of the parent compound of superconducting infinite-layer nickelates, [arXiv:1909.02678](https://arxiv.org/abs/1909.02678) [*Nat. Mater.* (to be published)].
- [21] K. Mikhalev, S. Verkhovskii, A. Gerashenko, A. Mirmelstein, V. Bobrovskii, K. Kumagai, Y. Furukawa, T. D'yachkova, and Yu. Zainulin, Temperature dependence of the sublattice magnetization of the infinite-layer antiferromagnet  $\text{SrCuO}_2$ , *Phys. Rev. B* **69**, 132415 (2004).
- [22] H. B. Radousky, A review of the superconducting and normal state properties of  $\text{Y}_{1-x}\text{Pr}_x\text{Ba}_2\text{Cu}_3\text{O}_7$ , *J. Mater. Res.* **7**, 1917 (1992).
- [23] A. I. Liechtenstein and I. I. Mazin, Quantitative Model for the Superconducting Suppression in  $\text{R}_{1-x}\text{Pr}_x\text{Ba}_2\text{Cu}_3\text{O}_7$  with Different Rare Earths, *Phys. Rev. Lett.* **74**, 1000 (1995).
- [24] W. E. Pickett and I. I. Mazin,  $\text{RBa}_2\text{Cu}_3\text{O}_7$  Compounds: Electronic Theory and Physical Properties, *Handbook on the Physics and Chemistry of Rare Earths*, edited by K. A. Gschneidner, Jr., L. Eyring, and M. B. Maple (Elsevier, Amsterdam, 2000), pp. 453–489.
- [25] L. C. Gupta, Superconductivity and magnetism and their interplay in quaternary borocarbides  $\text{RNi}_2\text{B}_2\text{C}$ , *Adv. Phys.* **55**, 691 (2006).
- [26] W. E. Pickett and D. J. Singh, New class of intermetallic borocarbides: Electron-phonon coupling and physical parameters, *J. Supercond.* **8**, 425 (1995).
- [27] M. Debessai, T. Matsuoka, J. J. Hamlin, J. S. Schilling, and K. Shimizu, Pressure-Induced Superconducting State of Europium Metal at Low Temperatures, *Phys. Rev. Lett.* **102**, 197002 (2009).
- [28] S.-T. Pi, S. Y. Savrasov, and W. E. Pickett, Pressure-tuned Frustration of Magnetic Coupling in Elemental Europium, *Phys. Rev. Lett.* **122**, 057201 (2019).
- [29] K. Schwarz and P. Blaha, Solid state calculations using WIEN2k, *Comput. Mater. Sci.* **28**, 259 (2003).
- [30] E. R. Ylvisaker, K. Koepf, and W. E. Pickett, Anisotropy and magnetism in the LSDA+U method, *Phys. Rev. B* **79**, 035103 (2009).

- [31] A. B. Shick, A. I. Liechtenstein, and W. E. Pickett, Implementation of the LDA+U method using the full-potential linearized augmented plane-wave basis, *Phys. Rev. B* **60**, 10763 (1999).
- [32] See Supplemental Material at <http://link.aps.org/supplemental/10.1103/PhysRevB.101.020503> where information is provided on the DFT method and several results beyond those in the Rapid Communication.
- [33] J. Kuneš and W. E. Pickett, Kondo and anti-Kondo coupling to local moments in  $\text{EuB}_6$ , *Phys. Rev. B* **69**, 165111 (2004).
- [34] The VCA was accomplished by replacing  $Z = 60$  of Nd by  $Z = 59.8$ . The small shift in  $4f$  levels is unimportant.
- [35] Q. Li, C. He, J. Si, X. Zhu, Y. Zhang, and H.-H. Wen, Absence of superconductivity in bulk  $\text{Nd}_{1-x}\text{Sr}_x\text{NiO}_2$ , [arXiv:1911.02420](https://arxiv.org/abs/1911.02420).
- [36] A. Fujimori, Electronic structure, magnetism, and superconductivity in infinite-layer nickelates, *J. Club Condensed Matter Phys.* (2019), doi:[10.36471/JCCM\\_December\\_2019\\_02](https://doi.org/10.36471/JCCM_December_2019_02).